Soft Matter

Ultrasoft silicone gels with tunable refractive index for traction force microscopy

Journal:	*Soft Matter*
Manuscript ID	SM-ART-01-2024-000016.R2
Article Type:	Paper
Date Submitted by the Author:	06-May-2024
Complete List of Authors:	Terdik, J.; Harvard University, School of Engineering and Applied Science Weitz, David; Harvard University, Department of Physics Spaepen, Frans; Harvard University, School of Engineering and Applied Sciences

Soft Matter

ARTICLE TYPE

Cite this: DOI: 00.0000/xxxxxxxxxx

Ultrasoft silicone gels with tunable refractive index for traction force microscopy.

J. Zsolt Terdik,*[a] David A. Weitz,[a,b,c] and Frans Spaepen[a]

Received Date
Accepted Date

DOI: 00.0000/xxxxxxxxxx

We formulate and characterize silicone gels near the gelation threshold with tunable refractive index, $1.4 < n < 1.49$, and small viscoelastic moduli, $G' \sim 1$ Pa, for use in traction force microscopy. The near-critical gels have low-frequency storage plateau moduli between 50 Pa and 1 Pa, with loss moduli that are more than fifty times lower at low frequencies. The gels are linearly elastic up to strains of at least 50%. The refractive index of the gel is tuned to eliminate spherical aberrations during confocal imaging thereby minimizing signal loss when imaging through thick gel substrates. We also develop an index-matched colloidal particle, stabilized by a silicone brush, that can be dispersed throughout the gel. These particles can be used to determine the deformation of the gel. The combination of mechanical and optical properties of these near-critical gels extends the lower limit of stresses that can be measured with traction force microscopy to single mPa values, while minimizing optical aberrations.

In traction force microscopy (TFM), the deformation of an elastic substrate is used to measure the forces applied to the boundary of the substrate, while visualizing the sample attached to it above.[1] Typically, a transparent polymer gel with calibrated elastic properties is used as a substrate. Tracer particles embedded within the gel are located and tracked with a confocal microscope, that is also used to visualize the sample above the gel. Traction force microscopy and related techniques,[1,2] have been used to measure a wide range of biological and physical phenomena, spanning orders of magnitude in stress, including single-cell traction stresses with magnitudes of 10 Pa and interfacial cracks of drying colloidal films with stresses as high as 100 kPa. This stress range, while spanning orders of magnitude, is nevertheless significantly larger than stresses encountered in the rheology of soft solids. An order of magnitude estimate of modulus G of soft solids with length scale L can be made by assuming the interaction energies are thermal, $G \approx k_B T/L^3$. For a prototypical soft material such as a hard-sphere colloid dispersion, individual micron-sized particles can be identified and tracked with a commercial confocal microscope as the material is deformed, providing rich structural and dynamical information on internal deformations that occur in response to applied stress.[3–5] However, the length-scale $L \sim 1\ \mu$m is set by the size of individual colloids and necessarily gives rise stress on the order of 1 mPa.[6] Extending TFM to this range of stresses would enable a variety of mechanical measurements that link the microscopic deformations visualized in 3D with the confocal microscope to the mPa-scale forces that couple to the deformation. However mPa-scale stress sensitivity in TFM requires compliant substrates and high-resolution imaging to ensure measurably large displacements of the tracers from which to infer the deformation. In addition to the limitation on the range of stresses that are measurable, existing elastic substrates are not typically index-matched to the immersion oil of the objective. This refractive index mismatch, combined with the thickness of gel, gives rise to spherical aberrations that degrade the spatial resolution when imaging the sample through the substrate using confocal microscopy.[7,8]

In this paper, we formulate and characterize *poly*-dimethyl-diphenyl-siloxane (PDPS) gels with independently tunable elastic modulus and refractive index. Mechanically, the gels exhibit true elastic solid response at low frequencies, with plateau storage moduli of single Pascals and loss moduli that are approximately fifty times smaller. Conveniently, the near-critical gels are mixed from commercially available components and require no synthesis. For traction force microscopy applications, we also synthesize colloidal tracers that are index-matched to the gel and stabilized by a PDPS silicone brush, allowing them to dispersed in the gel. Chemically, the gels differ from *poly*-dimethyl-siloxane (PDMS) by substitution of dimethyl side groups for diphenyl groups along a siloxane backbone. Given the chemical similarity to commercial PDMS formulations used in TFM including, for example, Sylgaard-184 and CY52-276, both from Dow Corning, we propose these PDPS gels as substitutes in existing TFM protocols based

[a] John A. Paulson School of Engineering and Applied Sciences, Harvard University, 9 Oxford Street, Cambridge, MA 02138, USA
[b] Department of Physics, Harvard University, Cambridge, MA 02138, USA
[c] Wyss Institute for Biologically Inspired Engineering, Harvard University, Boston, MA 02115, USA
* Corresponding author, E-mail: terdik@g.harvard.edu

on PDMS elastomers, especially in cases where a more compliant substrate is desired, or to reduce spherical aberrations that arise when imaging through thick gel substrates.

1 Single mPa sensitivity: mechanical and optical constraints

While there are several methods of determining the deformation in TFM,[9,10] the minimum stress resolvable by this technique can be estimated by considering a uniform applied shear stress across the elastic substrate with single-particle locating of the embedded tracers to determine the shear strain. For typical thickness of $h = 50\ \mu$m and spatial resolution of $\delta x = 50$ nm obtainable from single-particle locating centroid locating,[11,12] the minimal resolvable stress σ depends on the shear modulus $G^{'}$ of the gel as $\sigma = G^{'} \cdot (\delta x/h) = G^{'}/1000$. Hence, single-mPa stress resolution using TFM requires gels with tunable moduli approaching 1 Pa. Higher precision particle locating,[13,14] thicker samples, or averaging over multiple particle displacements would further increase the stress sensitivity.

To minimize optical aberrations, the gel should be transparent, index-matched to any tracers dispersed in the gel, and index-matched to the immersion medium for the microscope objective. Meeting all three criteria eliminates scattering, reflections, and, crucially, spherical aberrations associated with confocal imaging at depths exceeding the thickness of the polymer gel.[7,8] Here we consider glycerol immersion objectives[15] with a refractive index of $n_D = 1.45$ and formulate the PDPS gels for this target. Similar formulation chemistry based on PDPS polymers outlined here can be used to prepare gels with a refractive index in the range of $1.4 < n < 1.49$. In particular, an ultra-soft gel without any diphenyl substitution will have $n = 1.40$. When paired with silicone oil immersion objectives available from Olympus, these gels would eliminate spherical aberrations and closely match the average refractive index of live cells. The higher limit of $n = 1.49$, achieved at the highest diphenyl substitutions commercially available would be similarly suitable for oil immersion objectives.

2 Gelation chemistry and formulation

The functional components of PDPS gels are vinyl-terminated and hydride-functional PDPS polymers that undergo a platinum-catalyzed hydrosilylation reaction.[16,17] The functional polymers are dispersed in a non-reactive polymeric liquid filler prior to the addition of a room temperature active catalyst. The refractive index of the gel is determined by the average phenyl content of the mixed components. The compliance of the gel is controlled by the cross-link density, which determines the mesh size of the gel. We use a combination of techniques to lower the cross-link density: use the highest molecular weight reactive pre-polymers that can be solubilized in the nonreactive liquid filler; use vinyl reactive polymers with functional end groups; use a polymeric cross linker; and use mass fractions of nonreactive liquid filler that approach the gel point.[18] These techniques lower the cross-link density, and thereby the modulus, while maintaining a fixed ratio of the reactive hydride and vinyl components. Once the reactive chemistry and molecular weight of the pre-polymers is determined, we can tune the refractive index by altering average phenyl content of the liquid filler and crosslinked network. By tuning the amount of liquid filler, we can tune the modulus. Hence, importantly, the mechanical and optical properties of the gel can be varied independently.

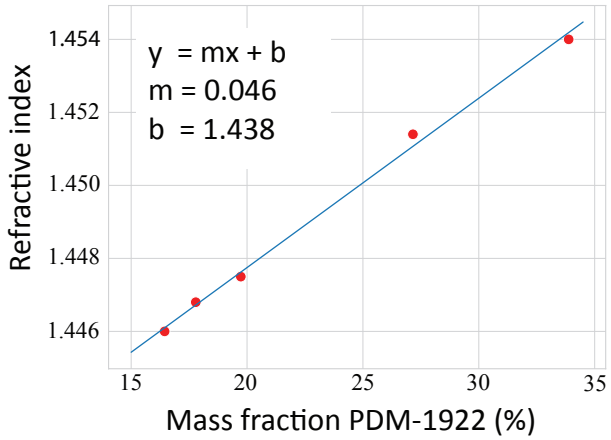

Fig. 1 Refractive index, measured with an Abbe refractometer, of two soluble non-reactive silicone oils (PDM-0821 and PDM-1922, Gelest) as function of weight percent PDM-1922. The target refractive index $n_D = 1.45$ occurs at 26 wt.% PDM-1922. Ordinary least squares regression (blue line) of the measured values (red points) is used to obtain slope and intercept values of 0.046 and 1.438 respectively.

The solvent compatibility of PDPS gels is similar to the solvent compatibility of PDMS gels, but depends on the diphenyl substitution.[19] Solvent compatibility of the gels can be quickly assessed by phase separation of the liquid filler with the solvent. Methanol, formamide and an aqueous solution of 4M urea showed complete phase separation with the liquid filler, and hence did not swell the cured gels. Water, however, is not compatible with PDPS gels used in this work, but is immiscible with PDMS which lacks diphenyl substitution, and is used as substrate for cell culture and traction force microscopy[20]. The gels used in this work are designed to eliminate spherical aberrations using glycerol immersion objective. For live cell imaging, spherical aberrations are minimized with silicone oil immersion objectives which closely match the average optical properties of cells and fall within the tunable range of silicone elastomers without diphenyl groups. We suspect that gels with analogous mechanical properties maybe formulated using commercially available reagents, in particular vinyl terminated base polymers (e.g. Gelest DMS-V35), hydride functional polymeric cross-linker (e.g. Gelest HMS-301), and non-reactive silicone oils (e.g. Gelest DMS-T35) in place of the diphenyl substituted analogs used in this work. Apart from diphenyl substitutions, these materials would be comparable to the ultrasoft gels in this work and the near-critical gels in Ref.[18].

The PDPS gels are formulated in three steps: formulation of stock solutions containing reactive components in a nonreactive liquid filler, mixing of these stock solutions to prepare a pre-gel solution that contains all reactive components as well as additional nonreactive liquid filler, and curing of the pre-gel solution by the addition of catalyst. Five stock solutions are required and their

composition is given in Table 1: liquid filler (λ) with the target refractive index; base solutions (b_1 and b_2) of vinyl-terminated PDPS polymers with refractive index lower, and higher, than the target value; hydride terminated crosslinker solution (c); and platinum catalyst solution.

2.1 Liquid filler (λ)

A liquid filler stock solution is prepared by mixing two non-reactive PDPS oils (PDM-1922 and PDM-0821, Gelest) that have, respectively, a larger and a smaller refractive index than the target value. For solutions of these silicone oils, the refractive index near the target value for glycerol immersion objectives can be varied as a function of the fraction of the higher refractive index component, as plotted in Figure 1. This liquid filler solution serves as diluent for the remaining stock solutions, and will be added to the pre-gel solutions to tune the mass ratio of liquid filler. A stock solution of several hundred grams is mixed at the target mass ratio, and its refractive index is measured with Abbe refractometer. The final composition may need additional adjustments to account for lot-specific variations in the refractive index of the neat components.

2.2 Base solutions (b_1 and b_2)

A high molecular weight, vinyl-terminated diphenyl-dimethyl siloxane with refractive index above the target (PDV-1641, Gelest) is mixed with the liquid filler stock solution. Similarly, a vinyl-terminated polymer with refractive index below the target (PDV-0541, Gelest) is mixed with the liquid filler. The base solutions (b_1 and b_2) are slowly tumbled overnight to ensure adequate mixing of the viscous components. Dilution with liquid filler has the benefit of lowering the viscosity. The mass ratio of vinyl-terminated polymers in these base solutions is set, so that an even mixture of the two base solutions will yield a volume weighted average refractive index equal to the target value. Hence, the mass ratio used to prepare the base solution will vary depending on the lot-specific refractive indices of the neat polymer. Note, that due to the high molecular weight of these reactive polymers, they are not miscible with each other, so that calibration measurements of the refractive index, analogous to Figure 1, are not possible. Nevertheless, the base polymers are soluble in the liquid filler, and yield transparent pre-gel solutions. During gelation, they are expected to form a network of random co-polymers with an average refractive index equal to the target value. After gelation, a transparent gel is formed indicating the absence of phase separation during gelation.

2.3 Crosslinker solution (c)

Fourth, a polymeric, hydride-functional crosslinker (HDP-111, Gelest) is dispersed in liquid filler, such that equal masses of the two vinyl-base solutions and the crosslinker solution (c) yield hydride-to-vinyl molar ratios of ∼4-5. Hydride-to-vinyl mol ratios larger than one, corresponding to an imbalanced stoichiometry of the reactive components, are used to ensure that the vinyl-terminated components are fully reacted and incorporated into the network. In principle, this ratio can be adjusted to maximize the ratio of $G^{'}/G^{''}$ in the cured gel. Here, however, no significant variation was found and the ratio $G^{'}/G^{''}$ was greater than 50 at low frequencies, comparable to commercial PDMS formulations. The polymeric hydride-functional cross-linker is a minority component, making up about 1% by mass of c, and approximately 0.1% by mass of the final pre-gel solution. While at the lower concentrations of the fully mixed pre-gel solutions the crosslinker is soluble prior to gelation, the mass ratio used for the stock solution is beyond the solubility limit as evidenced by the cloudy stock solution. A more dilute solution of crosslinker could be prepared and used by re-appropriating liquid filler from either the base stock solutions, thereby creating more viscous base solutions, or by the final diluent step at the expense of a larger minimum liquid filler mass fraction. Instead of these alternatives we chose to mix the crosslinker solution, as needed, until a homogeneously cloudy solution is attained.

2.4 Catalyst solution

Finally, a room temperature catalyst (SIP-6832.2LC, Gelest) is dispersed at 10% by weight in the liquid filler. No inhibitors are used; addition of $\sim 10\ \mu$L of catalyst solution per gram of pre-gel solutions ($p = 10\ \mu$L/g) allows a work time of several minutes. Other platinum catalysts can be used for elevated temperature curing (SIP 6833.2, Gelest). Diethyl maleate can be added at ppm concentrations to extend the work time,[21] however we find that near the gel point, addition of inhibitors increases the time for complete gelation, with inconsistent results. Decreasing the catalyst concentration is the preferred method of increasing the work time. Decreasing the catalyst concentration from $p = 10\ \mu$L/g to $p = 7\ \mu$L/g increases the work time by an order of magnitude.

2.5 Mixing pre-gel solutions and calibration

Using these stock solutions, a range of pre-gel solutions with varying liquid filler content and hydride-to-vinyl ratios can be prepared; gel compositions are given in Table 2. We use convention of $b_1 : b_2 : c : \lambda$ to specify the masses (in grams) of the stock solutions. The first three components, (b_1,b_2, and c), are solutions of vinyl-terminated base, (b_1,b_2), and hydride-functional crosslinker, (c), that have been diluted with liquid filler, while the fourth component, λ, is additional liquid filler used to achieve the desired liquid filler mass fraction. Given the formulation of the stock solutions, for a mass ratio of $b_1 = b_2$, the refractive index of the gel solution is independent of the amount of liquid filler added. Using this convention and the formulation of the stock solutions listed in Table 1, we can compute the total liquid filler mass fraction, ℓ, as function of additional liquid filler λ:

$$\ell = \frac{(1-0.198)\cdot b_1 + (1-0.167)\cdot b_2 + (1-0.011)\cdot c + \lambda}{b_1 + b_2 + c + \lambda}, \quad (1)$$

where the numerical pre-factors correspond to the mass fraction of liquid filler in the stock solutions computed from the composition in Table 1. Finally, we compute the hydride-to-vinyl mol ratio, r, using the hydride equivalent weights, $h_{\mathrm{eq}} = 150$ for HDP-111 and vinyl equivalents per kilogram $v_{1,\mathrm{eq}} = 0.033$ and

Table 1 Composition of stock solutions.

Stock solution	Component 1	Mass of component 1 (g)	Component 2	Total mass (g)
Liquid filler (λ)	PDM-1922	26	PDM-0821	100
Base 1 (b_1)	PDV-1641	0.839	λ	5.032
Base 2 (b_2)	PDV-0541	1.002	λ	5.052
Crosslinker (c)	HDP-111	0.046	λ	3.173
Catalyst	SIP6831.2LC	0.10	λ	1.0

Table 2 Mass percent liquid filler and rheological calibration of near-critical silicone gels.

Liquid filler (wt %)	$b_1(g)$	b_2 (g)	c (g)	λ (g)	$G^{'}/G^{''}$ (Pa)	Comments
94.7	0.507	0.502	0.354	2.199	56/0.1	
95.2	0.999	0.993	0.702	5.141	20.6/0.1	
95.4	0.679	0.672	0.474	8.437	10.8/0.1	4.8 g of 94.7% pre-gel solution and 5.5g of λ
95.6	0.824	0.819	0.579	11.304	5.7/0.1	6.5 g of 95.2% pre-gel solution and 7.1 g of λ

$v_{2,\mathrm{eq}} = 0.027$ for PDV-1641 and PDV-0541 respectively:

$$r = \frac{(0.011 \cdot c) \cdot h_{\mathrm{eq}}}{(0.198 \cdot b_1) \cdot v_{1,\mathrm{eq}} + (0.167 \cdot b_2) \cdot v_{2,\mathrm{eq}})/1000} = 6.64 \cdot \left(\frac{c}{b}\right), \quad (2)$$

where the numerical pre-factors in the first equality correspond to the weight fractions of the reactive polymer in the stock solutions. In a simplified equation the ratio of base stock solutions can be set such that $b_1 = b_2 = b$ in order to fix the refractive index to the target. For the gels used here, $(b_1 : b_2 : c : \lambda) = (1 : 1 : 0.7 : \lambda)$ corresponding to $r = 4.6$ and $\ell = (2.3 + \lambda)/(2.7 + \lambda)$.

3 Synthesis of index-matched, PDPS-stabilized tracers

Index-matched tracer particles were synthesized by a modification of Kogan *et al*,[22] with PDPS stabilizing brushes and polymer composition of the particle consisting of *poly*-trifluoroethyl-*co*-methyl methacrylate (MMA/FEMA) in place of *poly*-methyl methacrylate (PMMA) in order to match the refractive index of $n_D = 1.45$.[23] A stock solution of low molecular weight PDPS polymers is prepared by combining PDV-0525 and PDV-1625 at a weight fraction of 51.43%. This solution has an average phenyl content to match that of the liquid filler used in the near-critical gel. Additionally a stock solution of methacrylate monomers is prepared by combining 19.594 g of 2,2,2-trifluoroethyl methacrylate (Sigma 373761) with 9.395 g of methylmethacrylate (Sigma, M55909). This monomer solution, when used in a dispersion polymerization step, produces polymer particles with target refractive index of $n_D = 1.45$.

Synthesis of the graft co-polymer. The first step is to prepare a graft copolymer of PDPS-*co*-MMA/FEMA. In a 250 mL round bottom flask, 1.536 g of the PDPS solution is combined with 50g of hexane and boiled under reflux for 45 minutes, and then flushed with Argon. Next, 0.307g of radical initiator, azobisisobutyronitrile (AIBN, Sigma 441090) is added under continuous flow of Ar. The solution is boiled under reflux for an additional hour at 70° C. Next, 2.5 g of the monomer solution is injected with a non-coring syringe. The reaction boils under reflux for 12 additional hours, after which it is allowed to cool to room temperature. The cooled product is transferred to centrifuge tubes and centrifuged at 10,000g for 15 minutes. The supernatant, containing the graft co-polymer, is retained and used as a stabilizer in the dispersion polymerization, while the sediment is discarded.

Dispersion polymerization of colloidal particles. The retained supernatant is weighed and additional hexane is added, if necessary, to obtain a total mass of 60 g. The superatant is added to a 500 mL round-bottom flask. The flask is heated to 70° C under reflux and continuous flow of Argon for 30 min. In a beaker, 0.08g of AIBN is dissolved in 6.87 g of monomer solution. Trace dye (Exciton, Pyrromethene 605) is dissolved in the solution to produce a deep cherry-red color. This solution is injected into the round-bottom flask and heated under reflux at 70° C for 12 hours. The position of the flask is adjusted relative to the heat bath so that top surface of the reactants is ∼1 cm above the surface of the heat bath. After 12 hours, the solution is transferred through a Whatman #4 filter into centrifuge tubes and washed with hexane. Unincorporated dye and unreacted reagents are removed by repeated centrifugation at 500g for 15 minutes, followed by replacement of the supernatant with pure hexane and redispersion of the colloidal particles. This process is repeated until the unincorporated dye is removed and the supernatant is transparent and uncolored. As a final step, the hexane is replaced with non-reactive silicone oil solution used in the gel formulation (i.e. stock solution λ), and the colloids are re-dispersed by repeated cycles of tumbling and bath sonication. Once the particles are dispersed, residual hexane is removed by rotary evaporation at 50° C under reduced pressure. Given the index match between the particles and the silicone oil, the resulting solution is homogeneously pink and transparent indicative of index matching between the silicone oil and the particles.

4 Rheological calibration

The gelation threshold is approximately 96% liquid filler by mass. Below this threshold, the gels exhibit a low-frequency plateau modulus that decreases as the liquid filler percentage increases as shown in Fig. 2. Even the most compliant gels prepared near the gelation threshold exhibit linear elastic response for strains in excess of 50%, as shown in Fig. 3. Pre-gel solutions are prepared with target liquid filler fractions that are above and

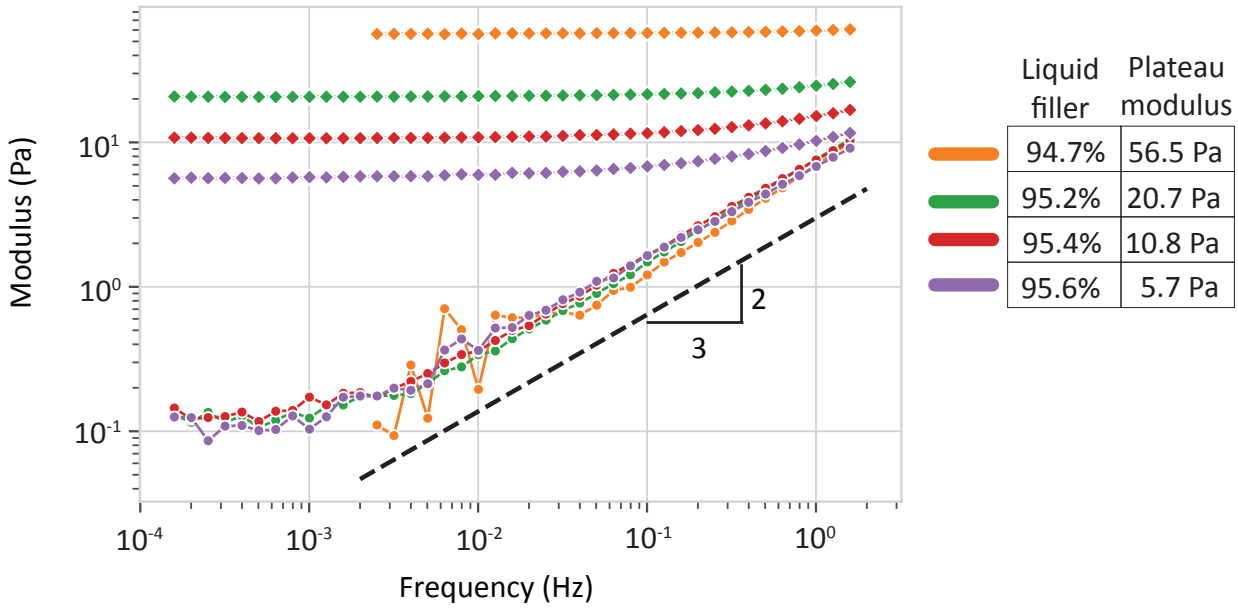

Fig. 2 Frequency sweeps of near-critical PDPS gels. The frequency-dependent viscoelastic moduli of PDPS gels show true solid behavior at low frequencies for a range of liquid filler fractions that approach the gel point. The storage modulus is plotted with diamond symbols, the loss modulus is plotted with circles, and the colors correspond to liquid filler fractions shown in the table. The plateau storage modulus at low frequencies spans an order of magnitude from 50 Pa to 5 Pa over a variation in liquid filler fraction of less than 1%. The frequency-dependent loss modulus shows a $\sim 2/3$ scaling exponent.

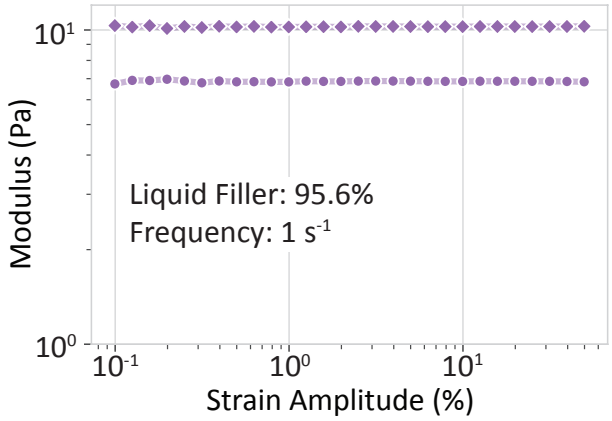

Fig. 3 Strain sweep of PDPS gels. The strain-sweep for the most compliant near-critical PDPS gel, measured at frequency of $f = 1\ \mathrm{s}^{-1}$, shows linear elastic behavior for strains up-to 50%.

below this threshold, as shown in Table 2. After tumbling the pre-gel solutions overnight, 10 μL of catalyst solution is added to 1 gram aliquots of the pre-gel solution, corresponding to a catalyst concentration of $p = 10\ \mu\mathrm{L/g}$, and tumbled by hand for 30 seconds. The gel solution is then loaded onto a strain controlled rheometer (Ares G2) with 50 mm parallel plate. Typical gap heights are 250-350 μm, and 25 μm trim gap. Rheological calibration steps are: (1) curing at 25° C while monitoring the gelation with small strain oscillation (1%) for 24 hours, (2) frequency sweep from 10 rad/s to 10^{-3} rad/s at fixed strain amplitude of 2%, (3) additional curing step for 12 hours, (4) additional frequency sweep, and (5) strain sweep from 0.1% strain to 50% at fixed frequency of 0.1 rad/s. As shown in Fig. 4, the time of G'/G'' crossover occurs at approximately 1000 seconds, with a full cure after 48 hours. Longer cure times with a typical crossover time of 10,000 seconds are achievable with a catalyst concentration of $p = 7\ \mu\mathrm{L/g}$.

The rheology tests on the two pre-gel solutions establish the upper and lower boundaries of the shear modulus. Any target shear modulus between these boundaries can be reached by mixing these pre-gel solutions at variable mass ratios, measuring the corresponding shear modulus, and iteratively adjust the mass ratio to obtain the target shear modulus. If the target shear modulus lies outside the boundaries, new upper and lower boundaries can be established using the existing pre-gel solutions, and treating pure liquid filler as the lower boundary. This is a simple process of *leapfrogging* in which a new lower bound is established by diluting one of the existing pre-gel solutions, preferably the pre-gel solution with higher shear modulus, with liquid filler. Once a pre-gel solution of the target shear modulus is measured, the remaining pre-gel stock solutions are mixed to the corresponding target mass ratio. Rheological calibrations are repeated on an aliquot of this pre-gel solution with a target mass ratio. If the modulus is unchanged, a third aliquot is prepared from which the TFM sample can be prepared and calibrated. In our experience, if the modulus is not reproducible or the gelation threshold occurs at liquid filler mass fractions that are more than a few tenths of a percent different from previous formulations, the most likely culprit is insufficient mixing of the stock and pre-gel solutions. This is especially true for the base solutions. If the sample does not gel, the most likely culprit is degradation of the catalyst solution. Pre-gel solutions that contain both vinyl and hydride groups, but lack

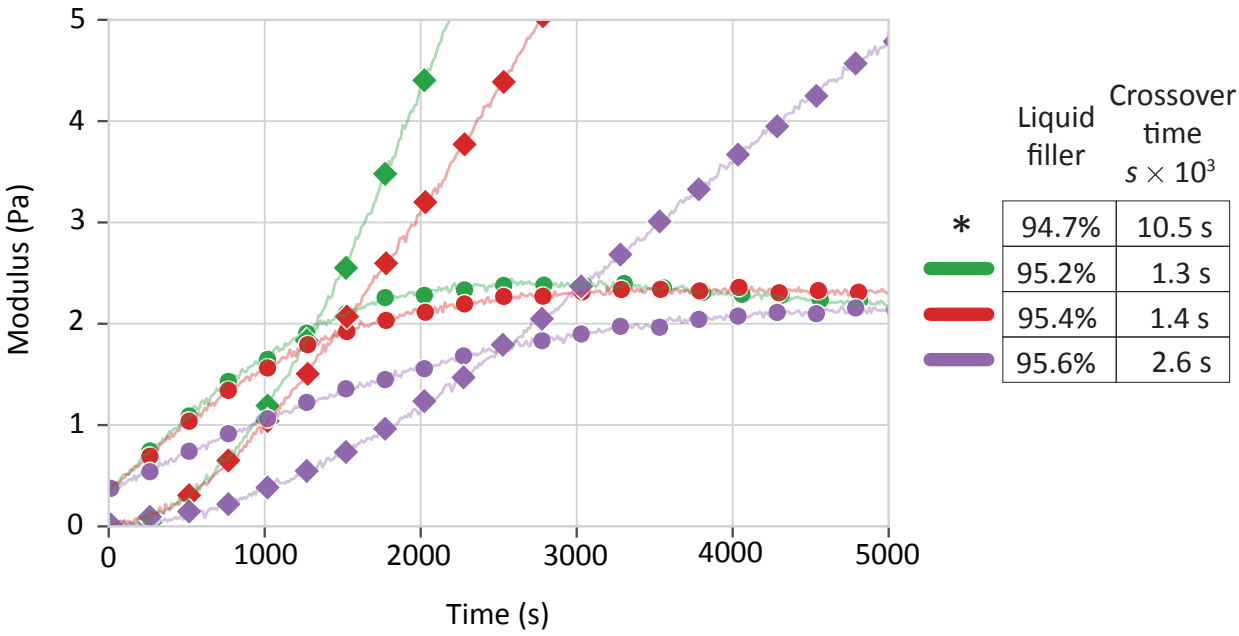

Fig. 4 Curing kinetics of PDPS gels. The curing time series shows the viscoelastic modulus at fixed strain and frequency during the gelation process. Every 20-th point in the curing time series is plotted with a circle for the loss modulus and diamond for the storage modulus. The crossover time, s, is the time at which the storage modulus first exceeds the loss modulus, and is a measure of the relevant work-time of the pre-gel solution after the addition of catalyst. It is on the order of 1000 seconds for catalyst concentration $p = 10\ \mu$L/g, corresponding to the addition 10 μL of catalyst solution per gram of pre-gel solution. A sample with liquid filler fraction of 94.7% (not plotted) was cured at lower concentration of catalyst solution, p=7 μL/g, and showed similar curing profile but with an order of magnitude slower crossover time of $s = 10.5 \times 10^3$ s, as shown in the table.

catalyst remain liquid for a month suggesting an absence of gelation. These pre-gel solutions can be used in subsequent dilution to achieve a lower modulus, followed by a rheological calibration of the diluted pre-gel solution.

5 Surface functionalization

The surfaces of the ultrasoft gels can be functionalized through a liquid deposition using solvents that are immiscible with the liquid filler. We have tested a deposition of *poly*-electrolyte multilayer, consisting of alternating layers of *poly*-styrene-sulfonate (PSS) and *poly*-diallydimethylammonium chloride (PDAC). 20 mM solutions of polyelectrolyte was prepared in formamide and syringe filtered. The layers were formed by sequential adsorption of the polyelectrolyte solution, followed by a 20 minute soaking period, and several washes of water. The surfaces showed similar adsorbing and non-adbsorbing behavior to glass surfaces treated.

6 Results and conclusion

The procedure outlined above was used to produce a series of gels with a low frequency plateau storage modulus between 50 Pa and 5 Pa as shown in Fig. 2. For catalyst concentrations of $p = 10\ \mu$L/g, the gels fully cure at room temperature in 36 hours. We observe no change in the frequency-dependent moduli after 2-3 day of additional curing. After 1 month of storage, the gels retain their clarity and ultra-soft compliance as they are visibly deformed under their own weight for $G < 5$ Pa. The gels behave as true elastic solids at low frequency ($G'/G'' > 50$ for $f < 10^{-3}$ s^{-1}) similar to that of commercial PDMS elastomers. Interestingly, the frequency-dependent loss modulus has a $\sim 2/3$ power law dependence, consistent with experimental studies on near-critical PDMS gels prepared with high molecular weight pre-polymers and liquid filler,[18] and theoretical predictions.[24–26] The strain sweeps, conducted at frequency of $f = 1$ s^{-1} show no variation in modulus up to strains of at least 50% as shown in Fig. 3. Based on these calibration results, a 5 Pa gel fabricated to 100 μm thickness can be used to measure stress over at least three decades: from 2.5 mPa to more than 2500 mPa based on the estimates of stress resolution with single-particle locating.

To demonstrate the optical quality attainable with these gels over commercial silicone gels, we created 145 μm thin layer of the PDPS gel and sedimented onto it a colloid dispersion of 1.6 μm diameter particles dispersed in formamide. Using a 63x glycerol immersion objective and spinning disk confocal (Andor W1) we see minimal signal loss even at depths of 150 μm as shown in Figure 5. By contrast, when a similar sample is prepared using commercial PDMS (Dow Corning, Sylgaard 184) as the substrate, the fluorescence intensity at the top surface of the elastic substrate is reduced threefold. Furthermore, there is deterioration in lateral and axial resolution at all heights in the sample above the gel. For these tests, the gels were prepared without tracers in order to rule out possible scattering from a dispersed phase. The loss in signal and spatial resolution is expected due to spherical aberrations caused by the refractive index mismatch between the commercial PDMS and the glycerol immersion fluid. These deleterious optical effects would be exacerbated with either water or oil immersion objectives, as these objectives have even larger refractive index mismatches.[7,8,15]

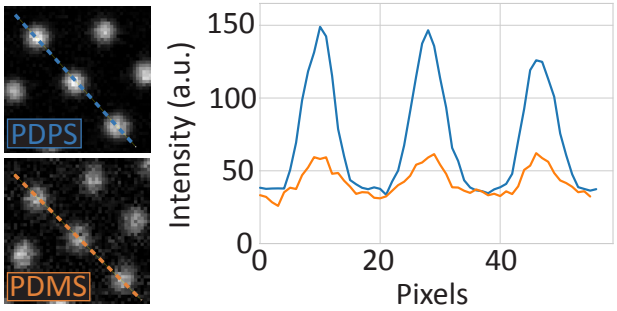

Fig. 5 Comparison of images of colloidal particles imaged through PDMS and PDPS substrates. To assess image quality, two substrates of PDMS and PDPS gels of thickness 145 μm are prepared and a colloidal crystal is deposited onto each substrate. The PDMS formulation (bottom row, Sylgaard 184) has refractive index of $n_D = 1.4$, while the PDPS gel presented in this work (top row), has refractive index of $n_D = 1.45$. The crystals are formed from an identical batch of particles and imaged under identical microscope parameters. Due to the refractive index mismatch between PDMS substrate and the glycerol immersion objective, the signal intensity measured through the center of the colloidal particle is degraded threefold (bottom row and orange curve) relative to the intensity achieved when imaging through PDPS substrates formulated to match the refractive index of the glycerol immersion medium (top row and blue curve).

In conclusion we present a formulation of near-critical polymer gels, and synthesis of tracer particles for use in traction force microscopy applications. The tunable refractive index allows adjustment of the optical properties of the gel to minimize optical aberrations when scanning through the thickness of the gel. The combination of an independently tunable refractive index and compliant moduli will enable new applications of TFM with thick, compliant substrates, with single mPa stress resolution.

Conflicts of interest

There are no conflicts to declare.

Acknowledgements

J. Zsolt Terdik acknowledges helpful conversations with Tom Kodger, Rodrigo Guerra, Adrian Pegoraro, and Zach Gault. This work was supported primarily by the Harvard MRSEC program of the National Science Foundation under award number DMR 20-11754.

Notes and references

1 R. W. Style, R. Boltyanskiy, G. K. German, C. Hyland, C. W. MacMinn, A. F. Mertz, L. A. Wilen, Y. Xu and E. R. Dufresne, *Soft Matter*, 2014, **10**, 4047–4055.

2 R. C. Arevalo, P. Kumar, J. S. Urbach and D. L. Blair, *PLOS ONE*, 2015, **10**, e0118021.

3 P. Schall, I. Cohen, D. A. Weitz and F. Spaepen, *Science*, 2004, **305**, 1944–1948.

4 P. Schall, D. A. Weitz and F. Spaepen, *Science*, 2007, **318**, 1895–1899.

5 K. E. Jensen, D. A. Weitz and F. Spaepen, *Physical Review E*, 2014, **90**, 042305.

6 H. M. Lindsay and P. M. Chaikin, *The Journal of Chemical Physics*, 1982, **76**, 3774–3781.

7 S. Hell, G. Reiner, C. Cremer and E. H. Stelzer, *Journal of microscopy*, 1993, **169**, 391–405.

8 A. Egner and S. W. Hell, in *Aberrations in Confocal and Multi-Photon Fluorescence Microscopy Induced by Refractive Index Mismatch*, ed. J. B. Pawley, Springer US, Boston, MA, 2006, pp. 404–413.

9 C. Franck, S. A. Maskarinec, D. A. Tirrell and G. Ravichandran, *PLOS ONE*, 2011, **6**, e17833.

10 B. Sabass, M. L. Gardel, C. M. Waterman and U. S. Schwarz, *Biophysical Journal*, 2008, **94**, 207–220.

11 D. Allan, T. Caswell, N. Keim, C. M. van der Wel and R. Verweij, *Genève: Zenodo*, 2021.

12 J. C. Crocker and D. G. Grier, *Journal of colloid and interface science*, 1996, **179**, 298–310.

13 M. Bierbaum, B. D. Leahy, A. A. Alemi, I. Cohen and J. P. Sethna, *Physical Review X*, 2017, **7**, 041007.

14 C. van der Wel and D. J. Kraft, *Journal of Physics: Condensed Matter*, 2016, **29**, 044001.

15 N. Martini, J. Bewersdorf and S. W. Hell, *Journal of Microscopy*, 2002, **206**, 146–151.

16 L. N. Lewis, J. Stein, Y. Gao, R. E. Colborn and G. Hutchins, *Platinum Metals Review*, 1997, **41**, 66–75.

17 J. Z. Terdik, D. A. Weitz and F. Spaepen.

18 J. C. Scanlan and H. H. Winter, *Macromolecules*, 1991, **24**, 47–54.

19 J. N. Lee, C. Park and G. M. Whitesides, *Analytical Chemistry*, 2003, **75**, 6544–6554.

20 R. N. Palchesko, L. Zhang, Y. Sun and A. W. Feinberg, *PloS one*, 2012, **7**, e51499.

21 L. N. Lewis, J. Stein, R. E. Colborn, Y. Gao and J. Dong, *Journal of Organometallic Chemistry*, 1996, **521**, 221–227.

22 M. Kogan, C. J. Dibble, R. E. Rogers and M. J. Solomon, *Journal of Colloid and Interface Science*, 2008, **318**, 252–263.

23 T. E. Kodger, R. E. Guerra and J. Sprakel, *Scientific Reports*, 2015, **5**, 14635.

24 M. Muthukumar, *The Journal of Chemical Physics*, 1985, **83**, 3161–3168.

25 M. Muthukumar, *Macromolecules*, 1989, **22**, 4656–4658.

26 J. E. Martin, D. Adolf and J. P. Wilcoxon, *Phys. Rev. Lett.*, 1988, **61**, 2620–2623.